Construction and Building Materials 226 (2019) 993–1005

Contents lists available at ScienceDirect

Construction and Building Materials

journal homepage: www.elsevier.com/locate/conbuildmat

Fracture and permeability properties of glass fiber reinforced self-compacting concrete with and without nanosilica

Yahya R. Atewi [a], Mustafa F. Hasan [b,*], Erhan Güneyisi [a]

[a] Department of Civil Engineering, Gaziantep University, 27310 Gaziantep, Turkey
[b] Department of Civil Engineering, Erbil Polytechnic University, 44002 Erbil, Iraq

HIGHLIGHTS

- The compressive strengths of SCC are mutually influenced by nanosilica content and glass-fiberfiber volumetric fractions.
- Increases in NS content between 0% and 4% result in increases in compressive strengths.
- The use of NS and GF provided an excellent enhancement in the static elastic modulus of SCC compared to those free of nS and GF.
- The flexural strength increased with increasing GF volume fraction.
- The added GF also improved the gas-permeability properties of each affected SCC mixture.

ARTICLE INFO

Article history:
Received 20 May 2019
Received in revised form 28 July 2019
Accepted 2 August 2019

Keywords:
Fracture energy
Permeability
Self-compacting concrete
Rapid chloride permeability
Glass fiber
Nanosilica
Fly ash

ABSTRACT

This article studied the influence of utilizing nanosilica (NS) and glass fiber (GF) on mechanical and permeability properties of self-compacting concrete (SCC) with fly-ash blended. There were three SCC series designed. This study had a constant amount of water-to-binder (w/b) ratio and total binder content which is 0.35 and 550 kg/m^3, respectively. This study utilized three different percentages of nanosilica to replace cement. These percentages were 0%, 2%, and 4% by weight, respectively. The incorporation of fly ash (FA) was done by using 25% of total binder content by weight in all the SCC mixtures. Moreover, glass fiber was used as an additive material with levels of 0%, 0.35%, 0.70%, 1.0%, and 1.5%, respectively. To experimentally evaluate mechanical properties; compressive strength; static modulus of elasticity; splitting tensile strength; fracture energy, and the permeability properties of the mixtures; sorptivity index; rapid chloride permeability test (RCPT); gas permeability test were done. The results showed that with utilizing nanosilica which ranged from 0% to 4% with replacement up until 0.7% glass fiber, indicated to enhance the mechanical and permeability properties of self-compacting concrete.

1. Introduction

In recent decades, there has been a significant rise in the improvement of the new age group of concretes. So, self-compacting concrete (SCC) is one of this development. In concrete production and concrete engineering, SCC is the newest development. Self-compacting concretes are composed of concrete mixes that possess properties that ensure compaction under their weight even without any extra handling. In other words, they are capable of filling the formwork even without segregation and de-aeration. There are concretes serve as an exceptional material for structures of concrete with multifaceted shapes or structures that require dense reinforcement. However, self-compacting concrete can be produced with the same raw materials that those of conventional way of concrete vibration. Self-compacting concrete needs too much quantity of superplasticizer so as to reduce water concrete and increase workability as much as possible. Moreover, self-compacting concrete must envelope high content of powder to reduce the frictional effect of coarse aggregate. Additionally, viscosity agents normally used to enhance concrete viscosity [1]. A few researchers demonstrate the possibility of the full replacement of recycled aggregates into self-compacting concrete (SCC). Even though the strength of recycled SCC is decreasing around 11% from the normal samples, in addition, the recycled concrete properties tend to improvement due to utilizing the optimum percentage of metakaolin. Furthermore, recycled concretes have higher apparent porosity and lower density than non-recycled concretes; therefore, they have more ability to absorb more water. On the other side,

* Corresponding author.
E-mail addresses: yahya.atewi@mail2.gantep.edu.tr (Y.R. Atewi), mustafafh9@gmail.com (M.F. Hasan).

https://doi.org/10.1016/j.conbuildmat.2019.08.029
0950-0618/

achieving lower density by using old cement paste, less wear resistance and more absorption in the recycled aggregate mixture compared to natural aggregates. In case the destruction aggregates of concretes which have less porous, the new concrete will absorb less water [45].

Detailed studies have shown that with the use of fibers, structural features of concrete include compression, bending, impact and tensile strength, as well as ductility and durability, which are significantly improved [2,3]. Among these fibers materials, glass fiber (GF) is cost-effective, lightweight and has high tensile strength. Studies have shown that by including these fibers, the destruction of shrinkage cracks and the bending and tensile strength of structural members can be achieved [4,5]. Increasing compressive strength when the use of nS up to 4%, while it decreases above 4% [6]. It was noted that increasing compressive strength and enhanced the fresh properties of SCC by using the fibers [7]. Basheerudeen and Anandan (2015) have observed with adding fibers the compressive strength increase significantly. The study also showed an increase in modulus of elasticity of SCC with fibers as compared to plain SCC is nearly 10% [8].

The concrete permeability is dependent on its pore structure. On the other hand, its electrical conductivity or resistivity depends on both the chemistry of the pore solution and the pore structure. Factors that are not directly involved with chloride transport can still greatly affect the concrete electrical conductivity. Therefore, in permeability properties, electrical conductivity or resistivity cannot be exploited as a symptom. Conversely, concrete's electrical conductivity or resistivity can still be used as a quality control indicator as long as the concretes have the same mixing proportions and components. However, utilizing the electrical conductivity of concrete as a direct indication of the ion's diffusivity is still not as feasible since these parameters are too difficult to evaluate. Nonetheless, different types of concrete or containing conductive materials able to characterized by rapid chloride migration test (RMT) which reported as a rapid and effective method. It was even proposed that it should replace the RCPT method [9].

Fly ash (FA) is one of the most utilized industrial wastes in the concrete and cement industry. As an additive, it has many advantages, such as increasing concrete's workability, reducing cement consumption, and potentially increasing concrete's mechanical strength and durability in the long run. Furthermore, different nano materials influence the concrete's mechanical performance and microstructure [10]. During the first 28 days, the addition of fly ash showed no significant effect on the self-compacting rubberized concrete's chloride ion permeability. However, by 90 days, it was revealed that there was a significant decrease in the entrance of chloride ions. This can be attributed to the fact that the long-standing of fly ash actually improves concrete's pore structure [11]. However, increasing fly ash resulted in decreased chloride permeability. The results also show that the higher substitution rate of fly ash and metakaolin leads to a decrease in the adsorption of concrete [12]. Moreover, there are two important concerns that arise when nanosilica in powder is used. The first issue lies in how the particles are dispersed at the mixing stage of the mortars or concrete. The second concern is the loss of workability because of the particles' high specific surface. Moreover, a few researchers presented that mechanical and flexural property of concrete, such as compressive strength, tensile strength, and flexural strength, and develop the cement microstructure according to the influence of filler with cement acceleration hydration during the nucleation effect. Therefore, the value can be rated as an optimum number with adding 1.5% montmorillonite nanoparticles through the high surface to volume ratio of nano-montmorillonite particle crystallites, we spoused that they will quickly respond with $Ca(H)_2$ and form calcium silicate hydrated (C-S-H) gel. In this reaction, the amount and size of calcium crystallites reduce and the consequential C-S-H improves the strength of samples by filling the empty spaces and increases the density of bond region (bond between cement matrix and sand) [13,14].

Adding nanosilica led to the enhanced compressive strength of HPSC across all ages. Strength development was seen to be at its greatest during the early curing ages mainly because of nanosilica's high pozzolanic activity during the initial periods. Furthermore, sorptivity and water absorption of HPSC decrease with increasing the nanosilica content. This is due to the fact that the concrete tends to become more compact, solid, and dense when the effects of pore filling and acceleration of hydration of nanosilica are combined. Moreover, it was observed that HPSC mixes that had 2% of nanosilica exhibited maximum water absorption and sorptivity values reduction. 2% nanosilica of HPSC had very low rapid chloride penetration test values at both 28 and 90 days. The nanosilica mixes were observed to pass lesser charges compared to the control mix. The significantly lower chloride-ion penetration can be attributed to the combination of circular particles like copper slag and nanosilica. This incorporation led to the enhancement of the matrix's element packing density [15]. The 90 days compressive strength is significantly increased when 5.0% NS and treated aggregate are used in combination [16]. Densification of the paste microstructures, especially those at the ITZ. SEM is a consequence of the pozzolanic response and the nano-filler effect of nano-silica. Based on observations, it was discovered that nanosilica-containing concrete had a more homogenous paste morphology at the ITZ. Moreover, concrete that had nano-silica showed increased water and chloride ion resistance as well as compressive strength, even at a low level of 0.3%. At this dose, uniform dispersion of silica nanoparticles can be easily achieved. Reductions of 45%, 31%, and 28.7% were observed for water penetration depth, chloride diffusion coefficient into concrete, and chloride migration coefficient, respectively. The nano-silica marginally changed the initial water sorptivity, water accessible porosity, and water absorption [17].

Bahari A. et al. (2018) reported that work, La $Sr_{0.5}Co_{0.5}O_3$ perovskite crystallites were synthesized with the sol-gel route. Then 1, 2 and 4 wt% of LSCO nanocrystallites, labeled to SN-1, SN-2, and SN-4, were directly incorporated into the cement paste matrix and studied their structural and mechanical properties with some related techniques. The EDS pattern, mechanical test, and data show an introduction of a relatively small amount of LSCO nanoparticles (2 wt%) into the cement matrix could enhance the flexural strength of LSCO/cement samples. Furthermore, as AFM and DM-SPM analysis demonstrated, the SN-2 sample has less surface roughness, fewer cracks, and more resistant structure compared to local lattice dislocation, suggesting that it can be used in the future cement-based material productions. Also, the results show that the SN-2 sample has a more stable mechanical structure and higher flexural strength due to the more occupation of the trap sites into the cement and diffusion of particles (crystallites) through the cell boundary and inside the cells [18]. The chloride-ion permeability test presented that the specimens at the ages of 28 and 56 days provided the lowest resistance to the chloride-ion permeability, garnering a 'medium' rating. Adding minerals clearly reveals an effective reduction in chloride ion permeability. Furthermore, this study was able to prove that even at 28 days, there is a reduction in the sorptivity index. Nonetheless, this effect was greater and more visible at 56 days. Concretes with the ternary blends of 5% SF and 30% FA showed the lowest sorptivity index at the 56 days testing age [19]. When mineral admixtures were used in concrete mixtures, concrete's chloride permeability showed significant reduction specifically at the 90 days testing age. As the substitution rate of FA or MK increases, the concrete with a binary blend of PC and FA or MK exhibits reduced chloride permeability. Concrete with a ternary mixture seems to be more

effective in building the resistance of concrete to chloride intrusion. Moreover, concretes that had mineral admixtures had lower sorptivity values at 28 and 90 days compared to the control concrete. There is a significant reduction in the sorptivity as the testing age increases from 28 to 90 days. This is partly due to the pozzolanic reaction that effectively decreases the pore space's volume. Furthermore, properties related to the strength and permeability, as well as durability, are improved when mineral admixtures are used in concrete production, especially for ternary blends like fly ash, Portland cement and metakaolin [20].

Nanoparticles can also be performed as a filler, working to improve concrete's density. In turn, this causes a clear decreasing in the concrete porosity. Nanoparticles not only act as activators, but also accelerate cement hydration due to their high activity, and they can also serve as the core in cement content. This results in smaller $Ca(OH)_2$ crystals and a more stochastic tropism. Utilisation of 2% NS in binary mixtures resulted in an increase in the compressive strength for binder content of 400 and 500 by 22%, 38% and 43%, 22%, 56% and 62% at 7, 28 and 90 days, respectively. In ternary mixtures, the compressive strength increased for binder content of 400 and 500 by 62%, 52% and 55%, 30%, 67% and 73% at 7, 28 and 90 days, respectively, when replacement by 10% SF and 2% NS was done. In binary mixtures, improvement in the compressive strength was greater in the mixtures that contained 2% NS. The highest improvement was observed in ternary mixtures. Generally, in all ages (7, 28 and 90 days), increasing the binder content led to increasing trends in compressive strength values. The decrease in water absorption for samples containing 2% NS in the first time step was discovered to be at 35% and 32% for binder content of 400 and 500, respectively [21]. The specimens' compressive strength increased when up to 4 wt% NS, 3 wt% NC, and 2 wt% NF were used, before display a reduction. An increase in the nanoparticle's content concentrated on the water absorption of the specimens. Additionally, the addition of nanoparticles significantly enhanced electrical resistivity. Adding NS, NF and NC reduced chloride permeability values by 60%, 44%, and 44%, respectively. The SEM micrographs as well exposed that the addition of nanoparticles led to smaller pores. This experiment can help develop the durability, mechanical, and microstructural properties of the SCMs mixtures [22]. Mixtures with 2% NS + 10% SF led to water absorption reduction at levels of 46% and 50% for binder content of 400 and 500, respectively. This indicates the good performance of SF + NS blends in the HPSCC mixtures. There was also a moderately clear reduction in the chloride ion percentage when SF and NS were added. This can be qualified to the concrete's more advanced pore structure that was achieved when admixtures were added, especially the material's nanoparticles and pozzolanic effect [21]. Based on E. Güneyisi et. al. (2019) utilizing of NS as replacement cement in quantities of 0%, 2%, and 4% with an unvarying fly ash inclusion of 25%. Experiments were conducted to identify the characteristics of the mixtures in the context of slump flow diameter, T50 slump flow time, L- box height ratio, and V-funnel flow time. Also, the modified Bingham model was applied to data from the ICAR rheometer to gauge the rheological behaviour of the self-compacting concrete. In addition, this study concluded that SCC with the replacement of 2% and 4% NS and maximum amount of GF achieved a lower rate of workability enhancement [46].

2. Experimental research

2.1. Resources

Portland-type cement (Portland CEM I42.5R) were utilized for this research which complies with TS EN197-1 standards largely derived from European EN197-1. These types exhibit blain-fineness of 326 m^2/kg and a specific gravity of 3.15 gm/cm^3, with chemical/physical properties as provided in Table 1. Additionally, admixtures of minerals such as NS measured 14 nm and pH values in 4% dispersions were from 3.7 to 4.7 as presented in Fig. 1. As well, class-F fly ash exhibited a specific gravity of 2.25 gm/cm^3 and a specified surface-area of 379 m^2/kg. Chemical composition and material characteristics for Portland cement, nanosilicas, and fly ash are shown in Table 1. Furthermore, GF has a glass content of 95% with properties as presented in Table 2 in terms of tensile strengths, lengths, diameters, and specific gravity, corresponding to 3400 MPa, 12 mm, 13 μm and 2.60 gm/cm^3 as presented in Fig. 2. The stones utilized were ground into coarse aggregates with maximum sizes of about 16 mm nominal, and also into medium aggregates with maximum sizes of 10 mm. Fine aggregates composed of naturally-occurring river sands with maximum sizes of 5 mm were utilized. The gradations in particle sizing acquired via analyses of sieved contents and the material properties of each fine and coarse aggregate mixture are shown in Table 3, with the usage of a superplasticizer (SP) with a specific gravity of 1.07 kg/cm^3 in each mixture as shown in Table 4

2.2. Proportions of the mixtures

In this research, 15 self-compacting mixtures of concretes were produced, covering a span of distinct mixtures featuring constant w/b ratios of 0.35 and collective binder contents of 550 kg/m^3. NS replacement of cement with fixed FA followed the different 0%, 2%, and 4% levels established for NS, while different 0.0%, 0.35%, 0.70%, 1.0%, and 1.5% levels were established for GF. Fixed replacement levels of 25% by the total mass of binder contents

Table 1
Chemical composition and physical properties of cementitious materials used.

Item	Portland cement	Fly ash	Nanosilica
CaO (%)	62.58	4.24	–
SiO_2 (%)	20.25	56.2	≥ 99.8
Al_2O_3 (%)	5.31	20.17	–
Fe_2O_3 (%)	4.04	6.69	–
MgO (%)	2.82	1.92	–
SO_3 (%)	2.73	0.49	–
K_2O (%)	0.92	1.89	–
Na_2O (%)	0.22	0.58	–
Loss on ignition	3.02	1.78	≤ 1.00
Specific gravity (gm/cm^3)	3.15	2.25	
Specific surface area (m^2/kg)	326	379	150,000

Fig. 1. Silicon dioxide nano particles.

Table 2
Technical Specification of glass fiber (GF).

Tensile Strength	3400 MPa
Modulus of Elasticity	77 GPa
Application Temperature limits	−60 °C to +650 °C
Melting Temperature	1120 °C
Specific weight	2,60 gm/cm^3
Fiber Diameter	13 mikron
Fiber length	12 mm

Fig. 2. Glass fiber used in this study.

Table 3
Sieve analysis and physical properties of aggregates.

Sieve size (mm)	Fine aggregate	Gravel	
		Medium	Coarse
16	100	100	100
8	99.7	100	31.5
4	94.5	1	1
2	58.7	0	0.5
1	38.2	0	0.5
0.5	24.9	0	0.5
0.25	5.4	0	0.4
Fineness modules	2.79	4.99	5.66
Specific gravity (gm/cm^3)	2.66	2.7	2.72

Table 4
Properties of superplasticizer.

Name	Gelenium 51
Color	Dark brown
State	Liquid
Specific gravity (kg/cm^3)	1.07
Description	Modified polycarboxylic type of polymer
Recommended dosage	% (1–2) binder content

were established for FA in all admixtures. The particulars of the admixture proportions are provided in Table 5. For mixture ID, fly ash is symbolized as FA, whereas glass-fibers are symbolized as GF and nanosilicas are signified as NS. For instance, FA25GF0.35NS0 specifies a SCC admixture formulated with fly ash contents of 25%, glass-fibers of 0.35% and nanosilicas of 0%.

2.3. Concrete castings

It is critical for the mixing procedures to be exact in their sequence of materials for processing in the mixer as well as the required amount of time. Specialized batching and mixing processes were adhered to, as methodical sequences and durations are critical in reaching similarly homogenous and uniform mixtures during SCC production. In this system, each fine and coarse aggregate was dispensed into a powered revolving-pan mixer and left to mingle for 1 min into a homogeneous aggregate. This was followed by the addition of about 25% of the mix water, and the aggregate was left to mix further for another minute, after which it was allowed to absorb water for a minute. The powdery materials, i.e. the cement plus fly ash and/or nanosilicas, were subsequently dispensed into the soaked aggregate and mixed for an additional 2 min. For admixtures with no fibers, the remainder of the mix water including SP was then dispensed into the mixer. Following SP, the remainder of the water was dispensed into the mixer, and SCC products with no fiber were mixed for 3 min and then allowed a rest period of 2 min. The concrete was then mixed for another 2 min to finalize the process.

This same sequential process was applied for the mixtures of composites with fibers, excepting that the fibers were dispensed before the remainder of the mix water with SP. The composites which contained fibers were then mixed for 300 s and subsequently allowed a resting period of 120 s. Mixed composites with no fibers were mixed for a duration of 9 min. while those which contained fibers were mixed for a duration of 11 min, not counting rest periods.

2.4. Testing procedures

2.4.1. Permeability properties

2.4.1.1. Resistance to chloride ion penetrations. A rapid chloride-permeability test, or RCPT, was performed to indicate the capacity of the concretes to withstand penetrations of chloride ions, in accordance with AASHTO T277 [23]. Three samples of each composite were tested simultaneously on the 28th and 90th day. After their curing phases, samples were acquired from the center of each 100 × 200 mm cylinder, for conditioning as reported in AASHTO T277 [23]. A data-logging specialist recorded the currents distributing through the concretes during a 6-hour interval. A diagram of the test site is illustrated in Fig. 3a and b. Once the testing was ended after the 6-hour interval, the currents (amperes) against times (seconds) were charted for every mixture, and the areas beneath the curves were calculated to acquire the charge distributed (coulombs). AASHTO T277 [23] categorizes chloride permeabilities in concretes into five levels from 'High' down to 'Negligible' according to the coulombs. The outcomes displayed include the averaged measures from three samples. Testing was performed at the 28th and 90th age days.

2.4.1.2. Sorptivity indices. Sorptivity testing measures the rates of water taken into the pores of concretes. Two samples measuring Ø100 × 50 mm which were taken from the Ø100 × 200 mm cylinders were employed. Preparation of the samples and the testing procedures were performed in accordance with ASTM C1585-13 [24] during the 28th and 90th age days of curing. Fig. 4 depicts the testing setup.

2.4.1.3. Gas permeabilities. As recommended in RILEM TC 116-PCD [25], the CEMBUREAU technique was performed to determine the gas permeabilities of the concretes. Each was measured on Ø150 × 50 mm disc samples taken from the middle part of each Ø150 × 300 mm cylinder. Gaseous oxygen was utilized as the penetrating medium. Variant pressure levels between 150 and 500 kPa were utilized on the samples to accumulate minimum lateral pressures of 7 bar (0.7 MPa) in the rubberized hose. For the testing of permeabilities, once the 28th and 90th age days of curing were over, the samples were oven-dried to ensure each sample's mass did not change by more than 1%. The samples were then secured in closed boxes until testing was started. During each test age,

Table 5
Concrete mix proportion for 1 m^3, with all unit weights are (Kg).

Mix ID	w\b	PC	FA	NS	Water	Gravel		Fine aggregate	SP	GF
						Medium	Coarse			
FA25GF0NS0	0.35	412.5	137.5	0	192.5	384.3	384.3	768.5	5.5	0
FA25GF0.35NS0	0.35	412.5	137.5	0	192.5	384.3	384.3	768.5	6.05	9.1
FA25GF0.70NS0	0.35	412.5	137.5	0	192.5	384.3	384.3	768.5	7.15	18.2
FA25GF1.00NS0	0.35	412.5	137.5	0	192.5	384.3	384.3	768.5	7.69	26
FA25GF1.50NS0	0.35	412.5	137.5	0	192.5	384.3	384.3	768.5	8.79	39
FA25GF0NS2	0.35	401.5	137.5	11	192.5	383.3	383.3	766.6	7.14	0
FA25GF0.35NS2	0.35	401.5	137.5	11	192.5	383.3	383.3	766.6	12.08	9.1
FA25GF0.70NS2	0.35	401.5	137.5	11	192.5	383.3	383.3	766.6	13.18	18.2
FA25GF1.00NS2	0.35	401.5	137.5	11	192.5	383.3	383.3	766.6	14.28	26
FA25GF1.50NS2	0.35	401.5	137.5	11	192.5	383.3	383.3	766.6	15.93	39
FA25GF0NS4	0.35	390.5	137.5	22	192.5	382.4	382.4	764.7	20.88	0
FA25GF0.35NS4	0.35	390.5	137.5	22	192.5	382.4	382.4	764.7	21.99	9.1
FA25GF0.70NS4	0.35	390.5	137.5	22	192.5	382.4	382.4	764.7	23.62	18.2
FA25GF1.00NS4	0.35	390.5	137.5	22	192.5	382.4	382.4	764.7	24.72	26
FA25GF1.50NS4	0.35	390.5	137.5	22	192.5	382.4	382.4	764.7	26.37	39

(a)

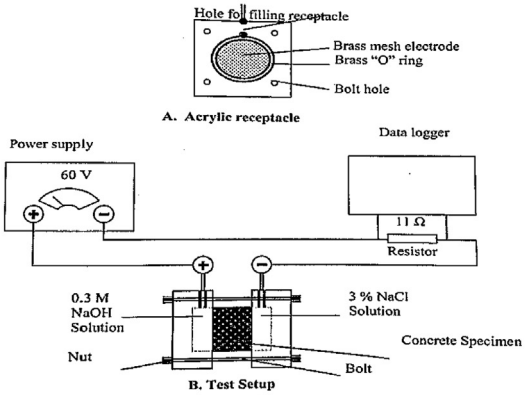

(b)

Fig. 3. a) Photographic view and b) schematic presentation of rapid chloride-permeability test (RCPT) (Gesoğlu and Güneyisi, 2011) [3].

three samples were examined and averages of their measures were registered. The diagram of the mechanism and details of the test compartment as well are presented in Fig. 5. For differential pressures between 150 and 500 kPa, the Hagen–Poiseuille correlation for laminar flows of compressed fluids via porous mediums

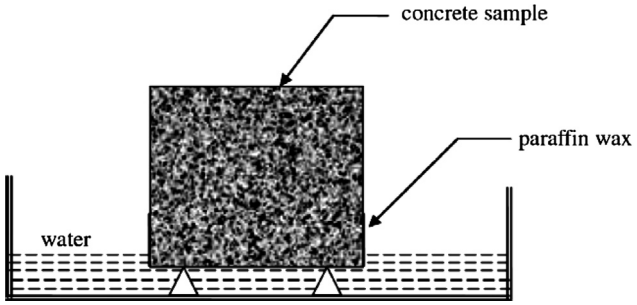

Fig. 4. Soptivity test set up (Güneyisi et al., 2015) [10].

containing minute capillary elements under steady-state conditions were utilized to resolve the evident gas permeability coefficient Kg, which is calculable through use of the modified Darcy formula shown in Eq. (1):

$$K_g = \frac{2P_2QL\mu}{A(P_1^2 - P_2^2)} \quad (1)$$

where K_g denotes the gas permeability coefficient (m^2), P_1 the ingress gas pressures (N/m^2), P_2 the egress gas pressures (N/m^2), A the cross-sectioned areas of the samples (m^2), L the heights of the samples (m), μ the oxygen viscosity (2.02×10^{-5} Ns/m^2), and Q the volumetric flow rates (m^3/s).

2.4.2. Mechanical properties

2.4.2.1. Compressive strength. Compressive testing was computed according to ASTM C39 (2012) [26]. The testing was likewise performed on three cubic forms measuring 150 × 150 × 150 mm by the 2000 capacity-testing device at 28 and 90 days.

2.4.2.2. Static modulus of elasticity. The static modulus of elasticity was determined on cylinder specimens, which is 150 × 300 mm as per ASTM C469 (2014) [27]. The modulus of elasticity is found by measuring the slope of the straight-line portion of the stress-strain curve.

2.4.2.3. Splitting tensile strength. According to ASTM C496 (2011) [28], splitting tensile strength was examined at 28 and 90 days. For this, three cylinder samples for each mixed examination, which dimension is Ø100 × 200 mm, though, It has been identified the splitting tensile strength (f_{st}) in MPa by Eq. (2).

$$fst = \frac{2P}{\pi dL} \quad (2)$$

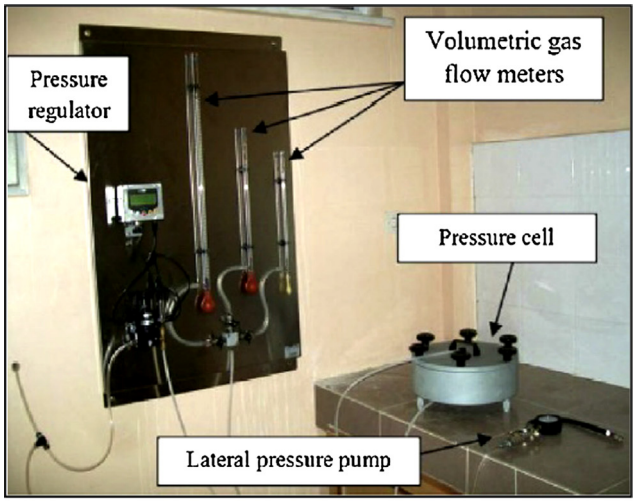

Fig. 5. Gas permeability details: a) photographic view of gas permeability device and b) detail of pressure cell.

where P, d, L is the maximum load in N, diameter in mm, and length of the cylinder mould correspondingly.

2.4.2.4. Fracture parameters. Many ways have been suggested by international standards to determine the fracture parameters. The simplest methods to calculate the fracture energy, as the greatest important fracture parameter of concrete, fracture energy was calculated by using work of fracture method introduced by the technical committee RILEM 50-FMC (1985) [29]. Prismatic specimens having 100 × 100 × 500 mm dimensions have been used. In this test, exhausting three-point bending test on notched prisms and determining the work wanted to generate a crack with unit surface area planned in a plane parallel to the crack direction, as the beam is broken in two parts, the specific fracture energy is calculated according to Eq. (3) [30]

$$G_f = \frac{W_f}{b(d-\alpha_0)} \tag{3}$$

where W_f, b, d, α_0 are total amounts of fracture works, a width of the beam, height of the beam, and notch depth, respectively. A closed-loop testing machine with a capacity of 250 kN was utilized to offer the load, Fig. 6a. Moreover, as shown in Fig. 6b, the ratio of the notch to depth (a/D) of the beam was 0.4, and the notch was created by sawing in order to accommodate large aggregates in more abundance decreased the effective cross-section to 60x100 mm. The span between two supports was 400 mm, and the mid-span deflection was calculated by a linear variable displacement transducer

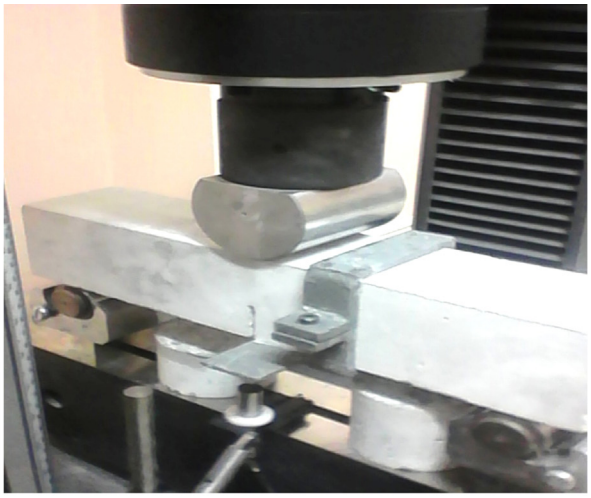

Fig. 6. a) Fracture test set up for the beam specimen, and b) Fracture energy relationship (Beygi et al., 2014) [30]

(LVDT). Also, net flexural strength (f_{flex}) providing from the notch beam, moreover, it was calculated as provided in Eq. (4).

$$f_{flex} = \frac{3P_{max}S}{2B(W-a)^2} \tag{4}$$

where P_{max} is fracture load, S is the span of beam, B is a width of beam, W is a depth of beam and a is a notch depth of beam. As well, it can be seen in Fig. 6b, the test is usually stopped at B, before the specimen is fully broken. Considering that the area under the ideal curve is intended and the effect must be eliminated, so proposed the following expression to calculate the area under the ideal load-displacement curve as calculated according to Eq. (5) [30].

$$W_f = W_m + 2\left(\frac{A}{u_B - u_A}\right) \tag{5}$$

where W_m is the area under the load-displacement curve which is corresponding to the surface area AMBA and A is a coefficient introduced.

3. Test results and analysis

3.1. Mechanical properties

3.1.1. Compressive strength

Compressive strengths are among the most vital mechanistic properties of concretes, which at times mirror the total performances of hardened concretes in terms of the service lives of structures. The result for each SCC composite with NS present

or absent at a different GF volumetric fraction is shown in Fig. 7a, b. Compressive strengths in the range of 67 to 84 MPa were attained in this research. The outcomes indicate that increases in GF at 0% to 0.7% volumetric fractions result in decreases in compressive strengths, while increases in GF up until a 0.7% volumetric fraction results in increases in compressive strengths for SCC composites comprising 0, 2% NS. Additionally to those SCC composites featuring 4% NS, increases in GF at 0% to 1.5% volumetric fractions resulted in increases in compressive strengths. Likewise, SCC compressive strengths increased with increases in NS content from 0% to 4%. The addition of 1, 2, 3, 4 and 5 wt% of nanoparticle elements, examined the durabilities of self-compacting mortars which contain nano-SiO_2, nano-Fe_2O_3, and nano-CuO, and stated that samples which contained 4 wt% NS manifested the maximum compressive strengths when compared to other samples [22]. The utilized 2, 4, and 6 wt% of nanosilicas in examining the fresh and rheological behaviours of nanosilicas and fly ash mixed into self-compacting concrete, and stated that NS utilisations of up to 4% increase the compressive strengths of SCC composites [31]. Embedded fibers afford concretes a way of halting growths in cracks and upgrading their load-carrying capacities. Moreover, increasing the amounts of glass-fibers results in decreasing incidences of cracks in SCC, producing increases in compressive strengths [32].

3.1.2. Static modulus of elasticity

Concrete. The variations in 90 days modulus of elasticity values of the SCC are plotted within Fig. 8 taking into consideration GF volume fractions. The modulus of elasticity values varied between 43.2 and 45.9 GPa, 46–49.3 and 47.8 and 50 GPa for concrete containing 0%, 2% and 4% NS, respectively. A comparison of the modulus of elasticity variation with that of compressive and splitting tensile strengths clearly shows a similar trend. The result of the present test shows that the SCC produced with 4% NS had a higher modulus of elasticity by 8%, 11%, 13%, 10% and 9% with 0, 0.35, 0.7, 1, and 1.5% GF, respectively, than those produced with 0% NS. On the other hand, the modulus of elasticity of SCC was increased with increasing GF volume fraction from 0 to 1.5% with different ratios of NS. Corinaldesi and Moriconi (2009) also observed the addition

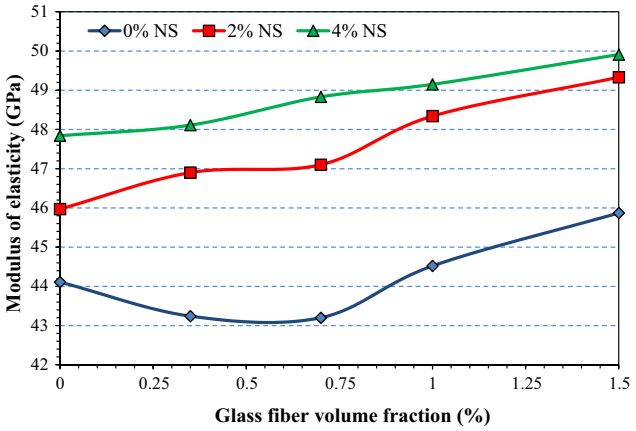

Fig. 8. 0Modulus of elasticity of GFRSCCs at 90 days.

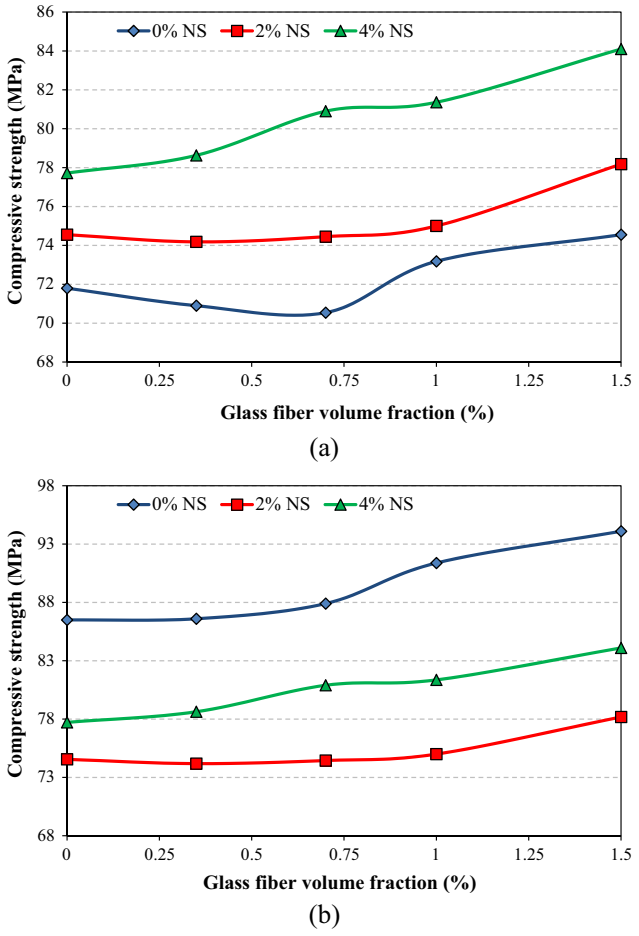

Fig. 7. Compressive strength of GFRSCCs at a) 28 days and b) 90 days.

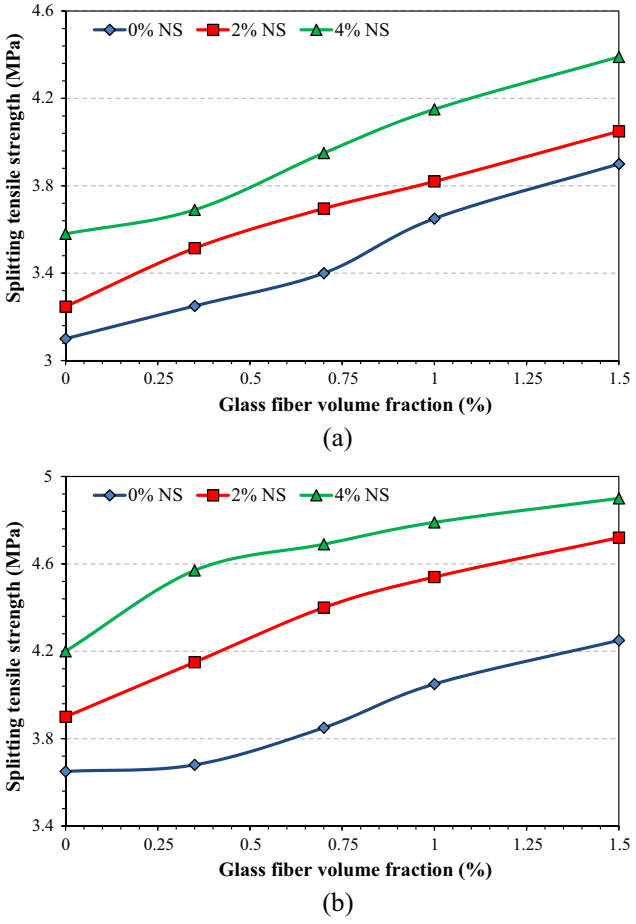

Fig. 9. Splitting tensile strengths of GFRSCCs at a) 28 days and b) 90 days.

of NS in concrete mixes improves the modulus of elasticity slightly due to increases in bonding between the aggregates and mortar. However, this enhancement is not so significant when compared with compressive strength as they reported [33].

3.1.3. Splitting tensile strength

The splitting tensile strength of SCC is much lesser than its compressive strength since it can be developed more rapidly with the propagation of cracks. Splitting tensile test method conducted herein covers the purpose of the tensile strength of cylindrical concrete specimens according to ASTM C496 (2011) [28], are graphically presented with respect to the five different volume fractions of GF (0%, 0.35%, 0.70%, 1.0% and 1.5%) in Fig. 9a and b for the 28 and 90 days curing period, respectively. It was clearly spotted from the figures that increasing of GF volume fraction leads to an increase in the splitting tensile strength of SCC. On the other hand, the result also indicated that the SCC produced with glass fiber gave the highest splitting tensile strength with deferent contents of nano-silica. For example, from the Fig. 9a the splitting tensile strength with 0% NS increased by 5%, 9%, 18% and 26% for SCC produced with 0.35%, 0.7%, 1%, 1.5% GF, respectively, in comparison to that of plain SCC. Similarly, the splitting tensile strength with 2% NS increased by 8%, 14%, 18%, and 25%, either using 4% NS, the splitting tensile strength increased by 3%, 10%, 16% and 23% at age of 28 days.

Furthermore, the result shows that the splitting tensile strength increases with increasing the NS content. In this regard, the maximum improvement in splitting tensile strength at 28 days due to the use of 2% and 4% NS is calculated as 9% and 16%, respectively, for SCC made with 0.7% GF. At the same line for those tested at

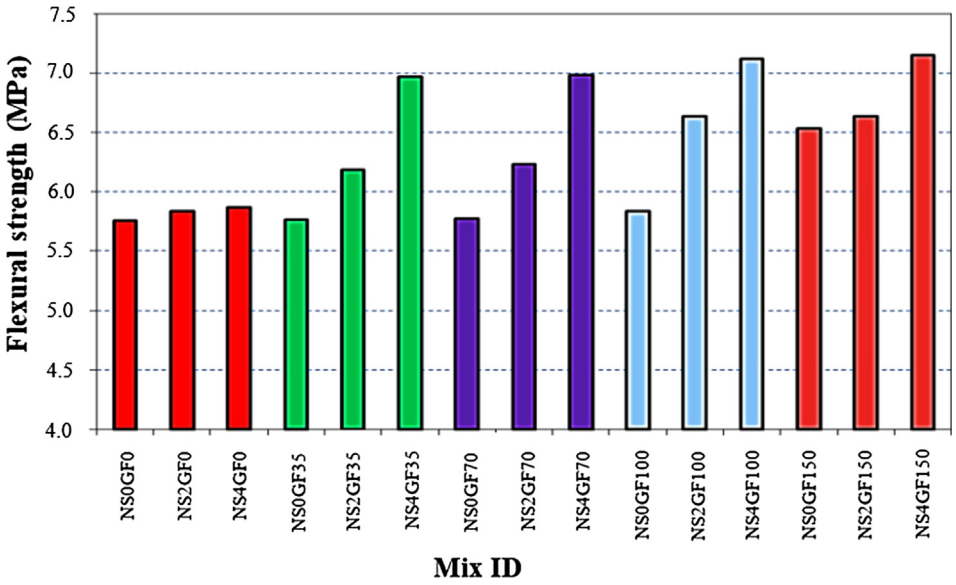

Fig. 10. Flexural strength of GFRSCCs.

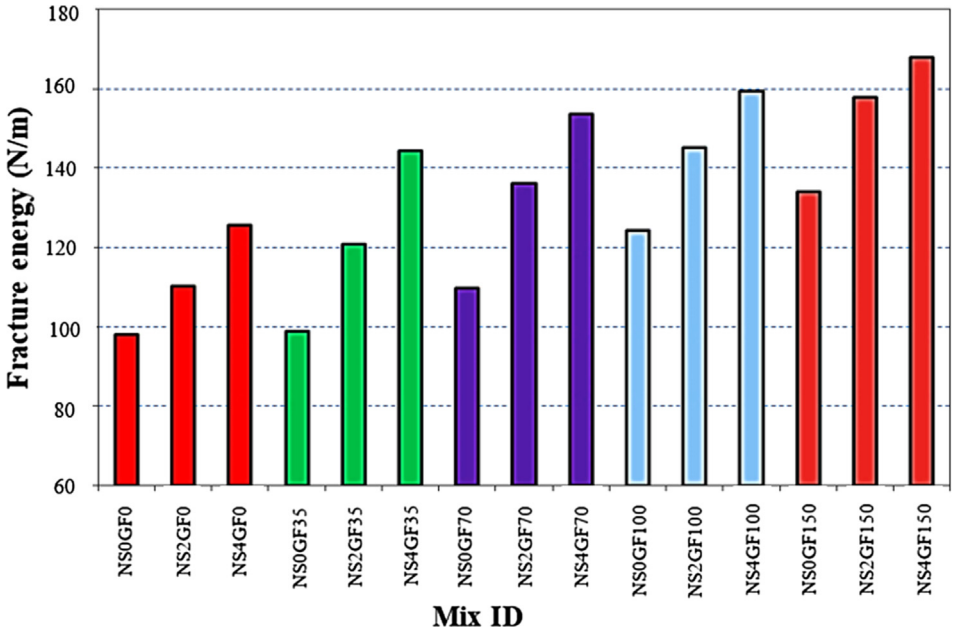

Fig. 11. Fracture energy of GFRSCCs.

90 days, the maximum percentage is computed as 14% and 24% for 2NSGF70 and 4NSGF35, respectively. Quercia et al., (2012) introduced an experimental investigation to study the mechanical and durability properties of self-compacting concrete containing precipitated silica in colloidal suspension or fumed powder NS were studied [34]. The percentage of NS was 3.8% by weight of cement. They reported that the splitting tensile strength after 28 days of curing was enhanced by about 21.51% and 9.91% for powder and colloidal NS, respectively. The development of denser and harder C-S-H gel due to the addition of NS improves the interfacial transition zone cause to improve the tensile strength of concrete [35].

Depend on the results, the splitting tensile strength of GFRSCC increases with increasing the GF volume fraction up to 1.5% and NS up to 4%.

3.1.4. Fracture parameters

Net flexural strength found from a three-point bending test on the notched specimen with respect to the volume fraction of GF is shown in Fig. 10. The GFRSCC with and without NS mixes had net flexural strength varying from 5.76 to 7.15 MPa. The highest value of the net flexural strength was observed in SCC mixture made with 4% NS and 1.5% GF as 7.15 MPa. The net flexural strengths of SCC without fiber were 5.76, 5.83 and 5.87 MPa at 0%, 2% and 4% NS contents, respectively. The enhancement in flexural strength due to the incorporation of GF and NS were found to be in the range of 6% to 14% and 19% to 22%, respectively. Kayali et al. (2003) reported that the main and major contribution of the fiber was due to the increase of tensile strain capacity of the concrete [36]. Gao et al. (1997) believed that the reason for increasing net flexural strength with the employment of fiber is that, after cracking of the matrix, the fibers will resist the load until the loss of the interfacial bond between the fibers and the matrix [37].

The fracture energy defined as the total energy dissipated over a unit area of the cracked ligament, representing the amount of work for the complete failure of a tested specimen [38]. The area under the curve of the load versus displacement is denoted as the energy necessary to break the material. Fracture energy was verifying versus GF volume fraction percentages at each of 0, 2 and 4% NS. The variation in fracture energy of SCC composites with and without NS at various GF volume fractions are graphically shown in Fig. 11. The result shows that the fracture energy increases with increasing GF volume fraction in all series. Moreover, the increase in the NS content leads to improve fracture energy of SCC. The figure obviously shows that the addition of GF had a significant effect on fracture energy. In this study the fracture energy for SCC mixtures ranging between 98 N/m and 168 N/m. Furthermore, the fracture energy with 0% NS increased by 1%, 12%, 27% and 37% with respect to SCC produced with 0.35%, 0.7%, 1%, 1.5% GF. While, the fracture energy with 2% NS increased by 10%, 24%, 32%, and 43%, either using 4% NS, the fracture energy by 15%, 22%, 27% and 34% at age of 90 days. On the other hand, the increase in content of NS without GF from 0% to 2% and 4% leads to an increase in fracture energy by 12% and 28%, respectively, while, the increase in fracture energy with 1.5% volume fraction of GF was 18% and 25%, respectively. Depend on the results, the fracture energy of SCC increase with the increase in GF and NS. In the study of Tavakoli et al. (2014), fracture parameters of SCC incorporating NS up to 6% were analyzed. They founded that the fracture energy magnitude increases with the increase of NS replacement level from 1% to 3% and then to decrease with the increase of NS content from 3% to 6%, thus, in terms of fracture energy they concluded that the optimum NS percentage is 3%. So, it can be said that the small amount of NS can be used to improve fracture energy and this should be related to the efficiency of NS. Typical loads versus displacement curves for SCC at 0%, 2% and 4% NS contents are given in Fig. 12a, b and c, respectively. These figures exhibited that the addition of GF to SCC caused to increase in both the ultimate load and area under the load-displacement curve [39].

The characteristic length is often considered to be a concrete property, and it gives a degree of the ductility/brittleness of the concrete. According to Mehta and Monteiro (2006), normal vibrated concrete has a characteristic length between 200 and 400 mm and compared to high strength concretes and lightweight aggregate concrete this range can be considered higher [40]. The variation in the characteristic length for SCC made with various GF volume fraction and NS content is presented in Fig. 13. The results showed that the addition of GF to SCC lead to an increase in the characteristic length. Thus, it can be indicated that the incorporation of such fiber made concrete more ductile. The results also revealed that NS incorporating yielded higher

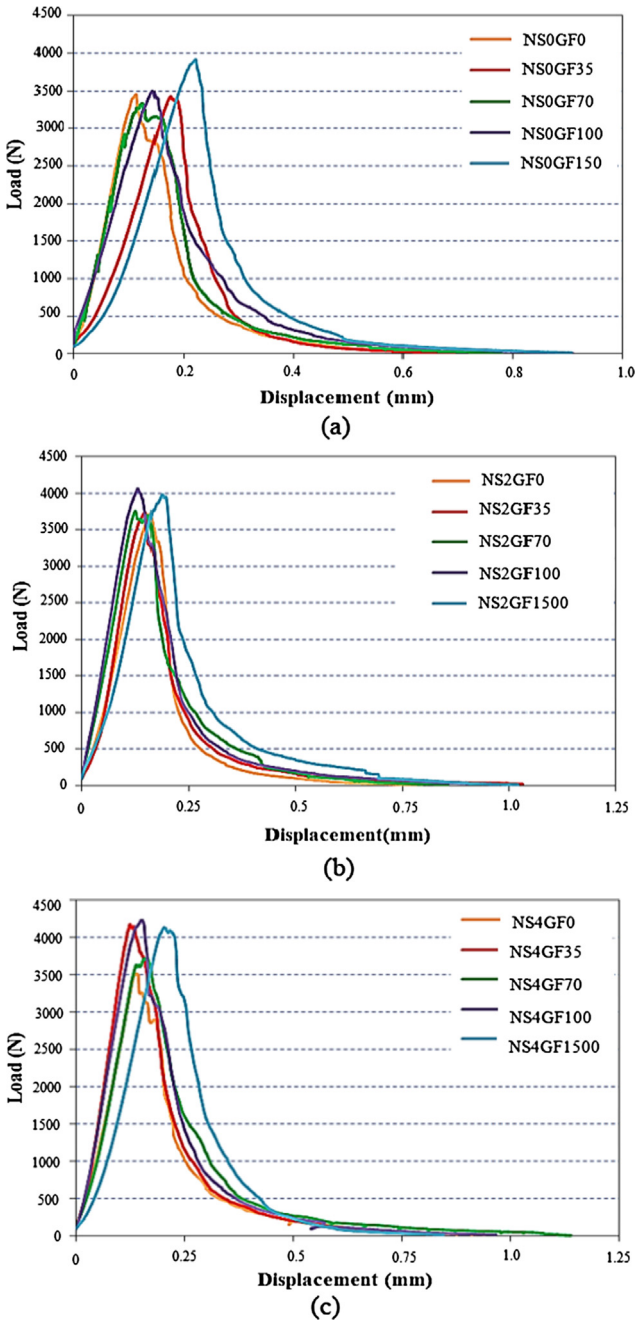

Fig. 12. Typical load versus displacement curves according to nS incorporation level: a) 0% NS, b) 2% NS and c) 4% NS.

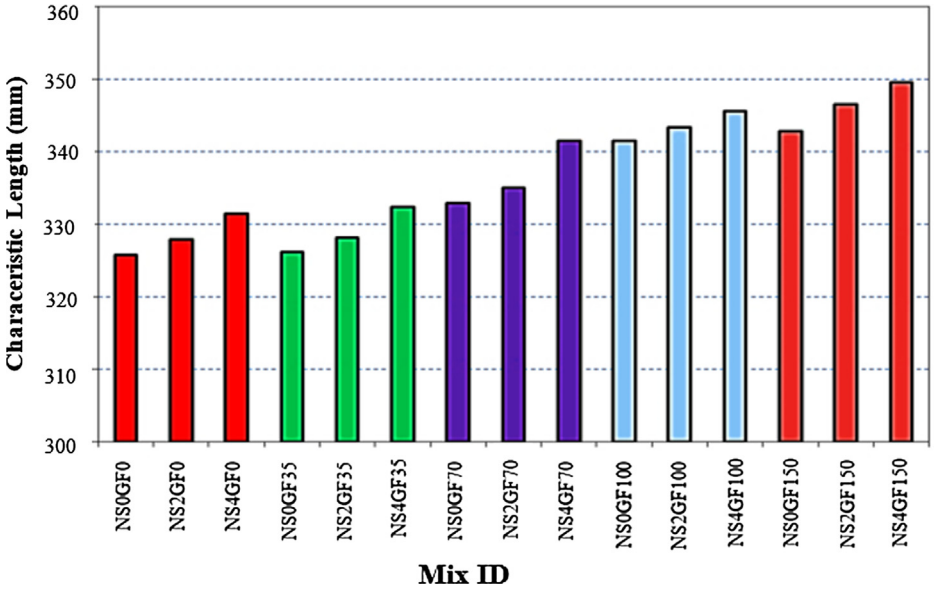

Fig. 13. Characteristic length of GFRSCCs.

characteristic length values. Thus, SCC composites made with NS are more ductile than the composite free of NS. The characteristic length of SCC with 4% NS was found to be higher than those of SCC with 0% and 2% NS content by 2% and 1%, respectively. The use of GF in SCC made it more ductile, this revealed from the increase in characteristic length for SCC made with GF. Furthermore, the characteristic length with 0% NS increased by 0.1%, 2%, 5% and 5% respectively for SCC produced with 0.35%, 0.7%, 1%, 1.5% GF. While, the fracture energy with 2% NS increased by 0.1%, 2%, 5% and 6%, either using 4% NS, the fracture energy by 0.3%, 3%, 4% and 5% at age of 90 days. This means that the brittleness of SCC decreases with the use of GF and NS.

3.2. Permeability properties

3.2.1. Chloride ion permeability

The entry of chlorides into concretes can induce damaging effects in reinforced steel. These are among the most critical issues found in concrete constructions around the world. The chloride-ion permeability test outcomes as functions of nanosilica and glass-fiber content as well as of test ages are illustrated in Fig. 14a, b. The information provided in Fig. 14 shows the chloride-ion permeabilities of the SCC composites range between 1370 and 3068 C and between 947 and 2694 C, corresponding to the 28- and 90-day periods. Gradual decreases in chloride-ion penetrations were observed with increases in GF volumetric fractions and NS content. In mixtures absent NS, with GF volumetric fractions increases from 0% to 1.5% chloride-ion penetrations showed decreases between 3068 and 3004 C, and between 2678 and 2578 C corresponding to the 28- and 90-day age periods. Additionally, mean reductions from 12.7% to 14.18% corresponding to 0%, 1.5% GF were seen with extensions of the curing periods to 28 and 90 days. As well, in mixtures comprising 2% NS content, chloride-ion penetrations showed decreases between 2299 and 1958 C, as well as between 1687 and 1547 C, corresponding to the 28- and 90-day age periods. For SCC composites comprising 4% NS content, chloride-ion penetrations showed decreases between 1452 and 1370 C as well as between 1002 and 958 C corresponding to the 28- and 90-day periods. These outcomes demonstrate the positive influence of GF and NS content increases on the chloride-ion permeability.

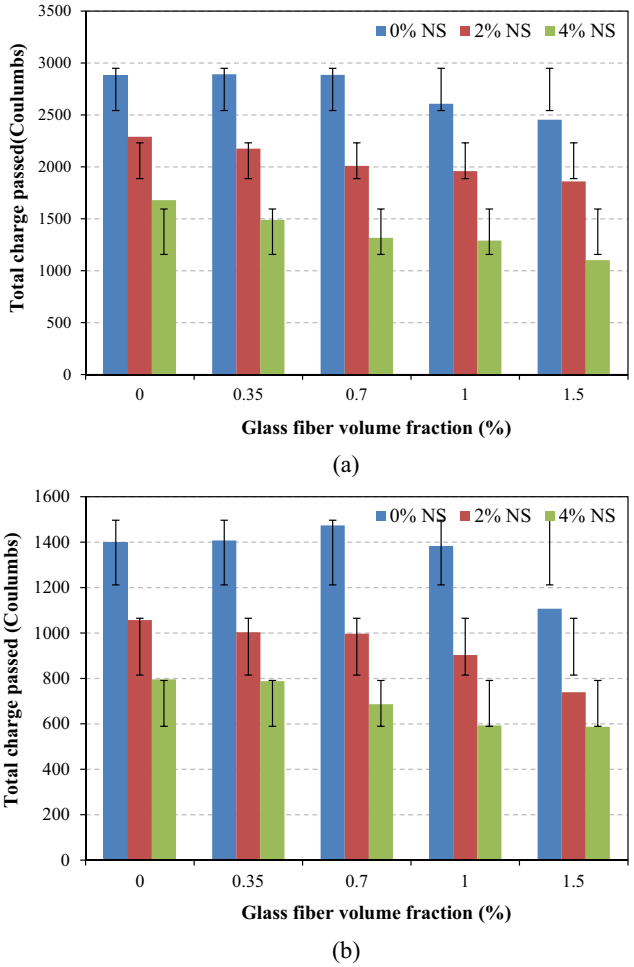

Fig. 14. RCPT test results; a) 28 days and b) 90 days.

3.2.2. Sorptivity index

The sorptivity of concrete surfaces is dependent on several aspects which involve the proportioning of concrete mixtures,

the occurrence of admixture chemicals and ancillary cementitious material, the physical constitution and properties of these cementitious materials as well as that of aggregate materials, the entrained air contents, the curing forms and durations, the hydration and aging levels, the incidence of micro-cracks, and the application of surface treatment types such as sealant or formation oils, and the positioning techniques involving consolidations and finishings. Absorption of water is also intensely influenced by the moisture levels in concretes at the point of evaluation [41]. The sorptivity coefficients of each glass-fiber self-compacting concrete composite according to its glass-fiber and nanosilica contents, along with test ages, are displayed in Fig. 15a, b. As observed, the sorptivity showed notable decreases with corresponding increases in nanosilica and glass-fiber content. For example, the mixture comprising 0% NS and 0% GF manifested a range of sorptivity coefficients between 0.0726 mm/min$^{0.5}$ and 0.07 mm/min$^{0.5}$ on the 28th day once the mixture comprised 1.5% GF. Likewise, increases in NS content between 0% and 4% at similar rates to glass-fiber of 0% resulted in corresponding decreases in sorptivity coefficients between 0.0726 and 0.0668. For every SCC composite, coefficient results calculated on the 90th day showed reductions in comparison to that calculated on the 28th day. The combining of NS into the SCC mixtures resulted in progressive reductions in their sorptivity coefficients, in correspondence with increases in their glass-fiber volumetric fractions between 0% and 1.5%. The sorptivities of the mixtures comprising 4% NS as well as 1.5% GF on the 90th day were averaging around 24.18% less than those calculated on the 28th day. These reductions did appear to be more significant in SCC composites with glass-fibers. At the 90th day age, the maximum values of sorptivity of 0.0686, 0.0625, and 0.0549 corresponded to mixtures NS0GF0, NS2GF0, and NS4GF0. As well, the lowest values of 0.0586, 0.0577, and 0.0486 corresponded to mixtures NS0GF1.5, NS2GF1.5, and NS4GF1.5. Several researchers have claimed that usage of NS enhanced the mechanical performances and durabilities of concretes in constructions, as the NS content enhanced the cement pastes owing to its superior pozzolanic characteristics, resulting in more finely hydrated stages (C-S-H gel) and densely arranged micro-structures [42,43].

3.2.3. Gas permeabilities

The permeabilities of SCC composite mixtures were ascertained to observe the influences of glass-fibers and nanosilicas on the durabilities of various concretes. This research utilized 0%, 2%, and 4% NS content in the replacements of cements, with different GF content ratios of 0%, 0.35%, 0.7%, 1%, and 1.5% volumetric fractions. The outcomes are depicted in Fig. 16a, b. The evident gas permeabilities of the concrete formed with GF fluctuated with the ingress pressures between 150 and 500 kPa. Also, a GF content of 0% obtained the maximum gas permeabilities in comparison to the corresponding GF ratios of 0.35%, 0.7%, 1.0%, and 1.5%. Determinations of the averaged values of the varied gas permeabilities accorded with the RILEM TC 116 (1999) [25] convention. Certain studies stated that their gas permeability testing acquired gas flows via measures of concrete porosities dependent on head pressures. This is dependent on the porosities of openings that dominate the materials examined. The porosities of the materials' capillaries were anticipated, with somewhat reliable correlations determined with gas permeabilities for the various SCC mixtures. Gas permeabilities for these mixtures are apparently far lower than for those of conventional concretes [44]. The disparities in values of gas permeabilities against GF and NS utilisations are presented in

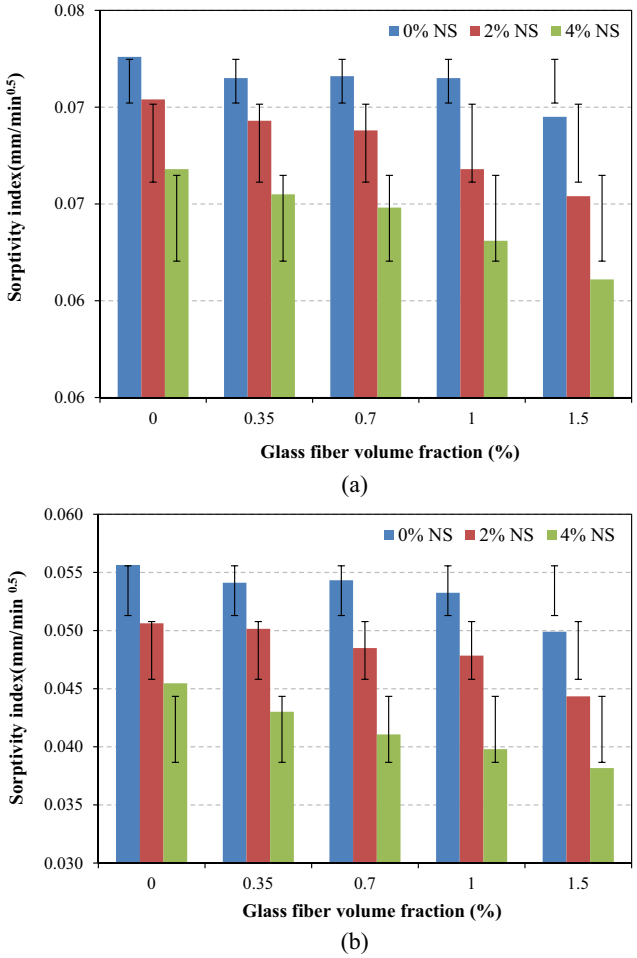

Fig. 15. Variation of the sorptivity index; a) at 28 days and b) at 90 days.

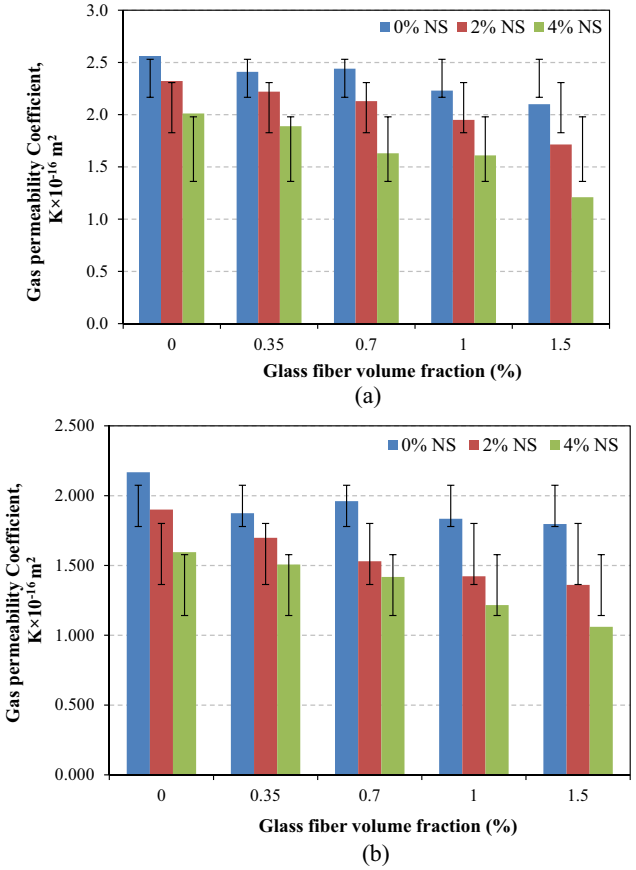

Fig. 16. Variation of apparent gas permeability; a) 28 days and b) 90 days.

Fig. 16. This research however established that decreases in gas permeabilities correspond to increases in the GF content ratios. The highest values of 0.71×10^{-16}, 0.58×10^{-16}, and 0.37×10^{-16} corresponded to the mixtures NS0GF0, NS2GF0, and NS4GF70. Conversely, the lowest values of 0.57×10^{-16}, 0.45×10^{-16}, and $0.3x10^{-16}$ (m^2) corresponded to 0, 2, and 4% NS content. More detailed information on GF and NS utilisation against changes in gas permeabilities is available.

4. Conclusions

This study presented the enhancement of self-compacting concrete properties, such as mechanical and fracture properties with utilizing glass fiber and nanosilica according to quantitative understanding. The following conclusions can be drawn from this study:

- The compressive strengths of SCC are mutually influenced by nanosilica content and glass-fiber volumetric fractions. Increases in NS content between 0% and 4% result in increases in compressive strengths. The added utilization of glass-fiber with rates between 0% and 0.7% results in decreases in compressive strengths of various SCC mixtures comprising 0% and 2% NS content. Compressive strengths increased with increasing percentages of glass-fibers up until 0.7%.
- The use of NS and GF provided an excellent enhancement in the static elastic modulus of SCC compared to those free of NS and GF and those modified with 0.35 and 0.70% GF. The key role of GF in improving the elastic modulus of concrete increased the efficiency of incorporated NS.
- The improvements of strength (compressive and splitting) were detected up to 4% of NS and 1.5% GF such that the maximum enhancement in strength of 34% was observed within 90 days splitting tensile strength of NS4%GF150 compared to that of the plain concrete.
- The flexural strength increased with increasing GF volume fraction. This is probably due to the fact that after cracking of the matrix, the fibers will resist the load until the loss of the interfacial bond between the fibers and the matrix.
- Through the work of fracture method, the fracture energy absorption capacity of SCC free of GF increases from 98 to 126 N/m and from 134 to 168 N/m for those of 1.5% GF as the NS content increased from 0% to 4%, respectively. Considering characteristics length, the incorporation of NS and GF leads to making SCC more ductile.
- The usage of nanosilicas and glass-fibers in SCC composite mixtures manifest substantial reductions in chloride-ion penetrations, as increases in GF volumetric fractions and NS content result in reduced chloride-ion penetrations. Moreover, average reductions of 12.7% and 14.18% corresponding to 0%, 1.5% were observed during the 28- and 90-day curing periods.
- From the analytical observations of the resulting variances, the sorptivity coefficients of the SCC mixtures showed decreases when GF volumetric fractions and NS content increased.
- The added GF also improved the gas-permeability properties of each affected SCC mixture. The evident gas permeability coefficients of the various SCC composites showed decreases when GF volumetric fractions increased. Furthermore, the addition of NS in various composites enhanced their gas-permeability behaviours as a productive result of improved pozzolanic activities and void-filling capability.

Declaration of interest

None.

References

[1] H. Okamura, Self-compacting high-performance concrete, Concr. Int. 19 (7) (1997) 50–54.
[2] RILEM TC188-CSC, Casting of self compacting concrete, Mater. Struct. 39 (10) (2006) 937–954.
[3] M.C. Alonso, M. Sanchez, C. Rodriguez, B. Barragan, Durability of SCC reinforced with polymeric fibres: interaction with environment and behaviour against high temperatures, in: 11th International Inorganic-bonded Fibre Composites Conferences, 2008, pp. 227–235.
[4] G. Barluenga, F. Hernández-Olivares, Cracking control of concretes modified with short AR-glass fibers at early age. Experimental results on standard concrete and SCC, Cem. Concr. Res. 37 (12) (2007) 1624–1638.
[5] F.A. Mirza, P. Soroushian, Effects of alkali-resistant glass fiber reinforcement on crack and temperature resistance of lightweight concrete, Cem. Concr. Compos. 24 (2) (2002) 223–227.
[6] A.S. Nik, O.L. Omran, Estimation of compressive strength of self-compacted concrete with fibers consisting nano-SiO_2 using ultrasonic pulse velocity, Constr. Build. Mater. 44 (2013) 654–662.
[7] M.M. Kamal, M.A. Safan, Z.A. Etman, B.M. Kasem, Mechanical properties of self-compacted fiber concrete mixes, HBRC J.. 10 (1) (2014) 25–34.
[8] A. Basheerudeen, S. Anandan, Simplified mix design procedures for steel fibre reinforced self compacting concrete, Eng. J. 19 (1) (2015) 21–36.
[9] C. Shi, Effect of mixing proportions of concrete on its electrical conductivity and the rapid chloride permeability test (ASTM C1202 or ASSHTO T277) results, Cem. Concr. Res. 34 (3) (2004) 537–545.
[10] A. Nazari, S. Riahi, The effects of SiO_2 nanoparticles on physical and mechanical properties of high strength compacting concrete, Compos. B Eng. 42 (3) (2011) 570–578.
[11] M. Gesoğlu, E. Güneyisi, Permeability properties of self-compacting rubberized concretes, Constr. Build. Mater. 25 (8) (2011) 3319–3326.
[12] E. Güneyisi, M. Gesoğlu, Z. Algın, K. Mermerdaş, Optimization of concrete mixture with hybrid blends of metakaolin and fly ash using response surface method, Compos. B Eng. 60 (2014) 707–715.
[13] A. Fujishima, X. Zhang, D.A. Tryk, TiO2 photocatalysis and related surface phenomena, Surf. Sci. Rep. 63 (12) (2008) 515–582.
[14] M.A. Kafi, A. Sadeghi-Nik, A. Bahari, A. Sadeghi-Nik, E. Mirshafiei, Microstructural characterization and mechanical properties of cementitious mortar containing montmorillonite nanoparticles, J. Mater. Civ. Eng. 28 (12) (2016) 04016155.
[15] S. Chithra, S.S. Kumar, K. Chinnaraju, The effect of Colloidal Nano-silica on workability, mechanical and durability properties of High Performance Concrete with Copper slag as partial fine aggregate, Constr. Build. Mater. 113 (2016) 794–804.
[16] E. Güneyisi, M. Gesoğlu, O.A. Azez, H.Ö. Öz, Physico-mechanical properties of self-compacting concrete containing treated cold-bonded fly ash lightweight aggregates and SiO_2 nano-particles, Constr. Build. Mater. 101 (2015) 1142–1153.
[17] H. Du, S. Du, X. Liu, Durability performances of concrete with nano-silica, Constr. Build. Mater. 73 (2014) 705–712.
[18] A. Bahari, A. Sadeghi-Nik, M. Roodbari, A. Sadeghi-Nik, Ebrahim Mirshafiei, Experimental and theoretical studies of ordinary Portland cement composites contains nano LSCO perovskite with Fokker-Planck and chemical reaction equations, Constr. Build. Mater. 163 (2018) 247–255.
[19] E. Güneyisi, M. Gesoğlu, E. Booya, K. Mermerdaş, Strength and permeability properties of self-compacting concrete with cold bonded fly ash lightweight aggregate, Constr. Build. Mater. 74 (2015) 17–24.
[20] G. Quercia, P. Spiesz, H.J.H. Brouwers, Effects of nano-silica (NS) additions on durability of SCC mixtures, in: Durability of Reinforced Concrete from Composition to Protection, 2015, pp. 125–143.
[21] M. Jalal, A. Pouladkhan, O.F. Harandi, D. Jafari, Comparative study on effects of Class F fly ash, nano silica and silica fume on properties of high performance self compacting concrete, Constr. Build. Mater. 94 (2015) 90–104.
[22] R. Madandoust, E. Mohseni, S.Y. Mousavi, M. Namnevis, An experimental investigation on the durability of self-compacting mortar containing nano-SiO_2, nano-Fe_2O_3 and nano-CuO, Constr. Build. Mater. 86 (2015) 44–50.
[23] ASHTOT277-89. American Association of State Highway and Transportation Officials. Standard Method of Test for Rapid Determination of the Chloride Permeability of Concrete, 444N. Capitol St., NW, Washington, DC 20001.
[24] ASTM C1585-13, Standard test method for measurement of rate of absorption of water by hydraulic-cement concretes annual book of ASTM standards, vol.04.02. American Society for Testing and Materials, 2014.
[25] RILEM TC 116-PCD, Permeability of concrete as a criterion of its durability, Mater. Struct 32 (1999) 174–179.
[26] ASTM C39/C39 M-12, American society for Testing and Materials. Standard test method for compressive strength of cylindrical concrete specimens. Annual book of ASTM Standard, 2012.
[27] ASTM. American Society for Testing and Materials, Standard Test Method for Static Modulus of Elasticity and Poisson's Ratio of Concrete in Compression (C469). Annual book of ASTM standards, vol. 04.02. West Conshohocken, Pennsylvania, USA, 2014.
[28] ASTM. American Society for Testing and Materials, Tensile strength of cylindrical concrete specimens (C496). Annual book of ASTM standards, vol. 04.02. West Conshohocken, Pennsylvania, USA, 2011.

[29] RILEM 50-FMC, Committee of fracture mechanics of concrete. Determination of fracture energy of mortar and concrete by means of three-point bend tests on notched beams, Mater. Struct. 18 (106) (1985) 285–290.
[30] M.H. Beygi, M.T. Kazemi, J.V. Amiri, I.M. Nikbin, S. Rabbanifar, E. Rahmani, Evaluation of the effect of maximum aggregate size on fracture behavior of self compacting concrete, Constr. Build. Mater. 55 (2014) 202–211.
[31] E. Güneyisi, M. Gesoğlu, A. Al-Goody, S. İpek, Fresh and rheological behavior of nano-silica and fly ash blended self-compacting concrete, Constr. Build. Mater. 95 (2015) 29–44.
[32] A.J. Majumdar, The role of the interface in glass fibre reinforced cement, Cem. Concr. Res. 4 (2) (1974) 247–268.
[33] V. Corinaldesi, G. Moriconi, Influence of mineral additions on the performance of 100% recycled aggregate concrete, Constr. Build. Mater. 23 (8) (2009) 2869–2876.
[34] G. Quercia, G. Hüsken, H.J.H. Brouwers, Water demand of amorphous nano silica and its impact on the workability of cement paste, Cem. Concr. Res. 42 (2) (2012) 344–357.
[35] B.B. Mukharjee, S.V. Barai, Influence of nano-silica on the properties of recycled aggregate concrete, Constr. Build. Mater. 55 (2014) 29–37.
[36] O. Kayali, M.N. Haque, B. Zhu, Some characteristics of high strength fiber reinforced lightweight aggregate concrete, Cem. Concr. Compos. 25 (2) (2003) 207–213.
[37] J. Gao, W. Sun, K. Morino, Mechanical properties of steel fiber-reinforced, high-strength, lightweight concrete, Cem. Concr. Compos. 19 (4) (1997) 307–313.
[38] K. Yu, J. Yu, Z. Lu, Q. Chen, Fracture properties of high-strength/high-performance concrete (HSC/HPC) exposed to high temperature, Mater. Struct. 49 (11) (2016) 4517–4532.
[39] H.R. Tavakoli, O.L. Omran, S.S. Kutanaei, Prediction of energy absorption capability in fiber reinforced self-compacting concrete containing nano-silica particles using artificial neural network, Latin Am. J. Solids Struct. 11 (6) (2014) 966–979.
[40] P.K. Mehta, P.J.M. Monteiro, Microstructure, Properties and Materials, third ed., McGraw-Hill, London, 2006.
[41] ASTM C1585-4, Standard test method for measurement of rate of absorption of water by hydraulic cement concretes, 100 barr harbor drive. PO Box C700, West Conshohocken (PA), 2004.
[42] Y. Qing, Z. Zenan, K. Deyu, C. Rongshen, Influence of nano-SiO_2 addition on properties of hardened cement paste as compared with silica fume, Constr. Build. Mater. 21 (3) (2007) 539–545.
[43] K. Sobolev, I. Flores, R. Hermosillo, L.M. Torres-Martínez, Nanomaterials and nanotechnology for high-performance cement composites, in: Proceedings of ACI session on nanotechnology of concrete: recent developments and future perspectives, 2006, pp. 91–118.
[44] V. Boel, K. Audenaert, G. De Schutter, Gas permeability and capillary porosity of self-compacting concrete, Mater. Struct. 41 (7) (2008) 1283–1290.
[45] A. Sadeghi-Nik, J. Berenjian, S. Alimohammadi, O. Lotfi-Omran, A. Sadeghi-Nik, M. Karimaei, The effect of recycled concrete aggregates and metakaolin on the mechanical properties of self-compacting concrete containing nanoparticles, Iran. J. Sci. Technol., Trans. Civ. Eng. 43 (2019) 503–515.
[46] E. Güneyisi, Y.R. Atewi, M.F. Hasan, Fresh and rheological properties of glass fiber reinforced self-compacting concrete with nanosilica and fly ash blended, Constr. Build. Mater. 211 (2019) 349–362.